PNAS RESEARCH ARTICLE | IMMUNOLOGY AND INFLAMMATION

Lymph-derived chemokines direct early neutrophil infiltration in the lymph nodes upon *Staphylococcus aureus* skin infection

Jingna Xue[a], Yujia Lin[a,b], Darellynn Oo[a], Jianbo Zhang[a], Ava Zardynezhad[a], Flavia Neto de Jesus[a], Matthew Stephens[a], Luiz G. N. de Almeida[c], Daniel Young[c], Antoine Dufour[c], and Shan Liao[a,1]

Edited by Melody Swartz, University of Chicago, Chicago, IL; received June 29, 2021; accepted May 27, 2022 by Editorial Board Member Tak W. Mak

A large number of neutrophils infiltrate the lymph node (LN) within 4 h after *Staphylococcus aureus* skin infection (4 h postinfection [hpi]) and prevent systemic *S. aureus* dissemination. It is not clear how infection in the skin can remotely and effectively recruit neutrophils to the LN. Here, we found that lymphatic vessel occlusion substantially reduced neutrophil recruitment to the LN. Lymphatic vessels effectively transported bacteria and proinflammatory chemokines (i.e., Chemokine [C-X-C motif] motif 1 [CXCL1] and CXCL2) to the LN. However, in the absence of lymph flow, *S. aureus* alone in the LN was insufficient to recruit neutrophils to the LN at 4 hpi. Instead, lymph flow facilitated the earliest neutrophil recruitment to the LN by delivering chemokines (i.e., CXCL1, CXCL2) from the site of infection. Lymphatic dysfunction is often found during inflammation. During oxazolone (OX)-induced skin inflammation, CXCL1/2 in the LN was reduced after infection. The interrupted LN conduits further disrupted the flow of lymph and impeded its communication with high endothelial venules (HEVs), resulting in impaired neutrophil migration. The impaired neutrophil interaction with bacteria contributed to persistent infection in the LN. Our studies showed that both the flow of lymph from lymphatic vessels to the LN and the distribution of lymph in the LN are critical to ensure optimal neutrophil migration and timely innate immune protection in *S. aureus* infection.

lymph flow | infection | neutrophil | lymph node | lymphatic vessel

Significance

An efficient innate immune response is essential in the host's immune protection during infection before adaptive immunity intervenes. We show that the earliest neutrophil infiltration to the lymph node via high endothelial venules is facilitated by lymph flow via delivering chemokines (i.e., Chemokine [C-X-C motif] 1/2 [CXCL1/2]) from the site of infection, which is much faster and more efficient than delivering lymphatic trafficking cells. Lymphatic dysfunction during skin inflammation impairs neutrophil migration and bacteria clearance. Our finding demonstrates the significance of lymph flow in innate immune protection and explains how preexisting inflammation conditions, such as dermatitis, can compromise lymph flow and result in higher risk and prolonged infections.

Skin and soft tissue infections (SSTIs) are the most frequent microbial skin infections in humans. Following a skin infection, neutrophils swarm around the invading microbes. Neutrophils can directly phagocytose and kill pathogens. Additionally, the activated neutrophils can release extracellular traps to immobilize pathogens, thus facilitating phagocytosis by other immune cells (1). These steps are critical to kill and restrain pathogens at the site of infection. However, some microbes may escape from the site of infection and travel through lymphatic vessels to the draining lymph node (LN) (2–5). Macrophages in the subcapsular sinus (SCS) are the first layer of LN-resident immune cells that capture these invading microbes (3, 6). Neutrophils rapidly infiltrate the draining LN to serve as a second layer of innate immune protection. Together, these macrophages and neutrophils in the LN play critical roles in preventing systemic pathogen dissemination (2, 5, 7). Depending on the type of microbial infection and the timing postinfection, neutrophils can infiltrate the LN from both high endothelial venules (HEVs) and lymphatic vessels (7–14). *Staphylococcus aureus* is one of the leading causes of SSTI, and methicillin-resistant *S. aureus* (MRSA) infection has become a worldwide health problem (15, 16). In *S. aureus* infection, neutrophils rapidly enter the LN via HEVs within 4 h postinfection (hpi) (7–10). How *S. aureus* skin infection can activate neutrophil recruitment from HEVs in the LN so quickly is not fully understood. Whether or not neutrophil lymphatic trafficking contributes to neutrophils recruitment via HEVs also remains unclear.

Lymph constantly flows from the skin to the LN for fluid balance and immune surveillance. During the first several hours postinfection, lymph composition changes rapidly, containing microbes, regulatory factors, and cell components. Tissue migrating dendritic cells (DCs) usually take several hours to activate and then, enter the LN via afferent lymphatic vessels (17). Lymph, however, only takes a few minutes to flow from infected skin via afferent lymphatic vessels to the draining LN. Thus, active lymph flow can rapidly "report" changes caused by the infection from the skin to the LN in a timely manner (4, 18). Whether and how the lymph flow from the skin to LN regulates neutrophil recruitment via HEVs remain unclear.

Within the LN, active lymph flow guides the distribution of lymph and its contents to designated locations (5). It is estimated that 90% of the afferent lymph flows from the SCS to the medullary sinus (MS) (19). Large molecules and microbes in the

Author contributions: J.X. and S.L. designed research; J.X., Y.L., D.O., J.Z., A.Z., F.N.d.J., L.G.N.d.A., D.Y., A.D., and S.L. performed research; J.X., Y.L., M.S., L.G.N.d.A., D.Y., A.D., and S.L. analyzed data; and J.X. and S.L. wrote the paper.

The authors declare no competing interest.

This article is a PNAS Direct Submission. M.S. is a guest editor invited by the Editorial Board.

Copyright © 2022 the Author(s). Published by PNAS. This article is distributed under Creative Commons Attribution-NonCommercial-NoDerivatives License 4.0 (CC BY-NC-ND).

[1]To whom correspondence may be addressed. Email: liaos@ucalgary.ca.

This article contains supporting information online at http://www.pnas.org/lookup/suppl/doi:10.1073/pnas.2111726119/-/DCSupplemental.

Published August 1, 2022.

afferent lymph are usually captured by CD169$^+$ SCS macrophages (6, 20–23) and SCS DCs (3). As such, most pathogens are restricted to the SCS after skin infection (2, 24). The activated SCS macrophages further secrete proinflammatory cytokines to activate and recruit other types of cells to the SCS (2, 25). The rest of the lymph can either diffuse or drain into the LN conduits to reach deeper into the LN. Lymph diffusion shows exponential decay from the sinus to 100 to 200 μm into the LN paracortex (B cell zone and interfollicular zone) and much less to the T cell zone (26). Conduit-mediated lymph drainage can rapidly reach HEVs in the T cells zone (27). LN conduits are composed of a core of extracellular matrix (ECM) proteins wrapped by fibroblastic reticular cells (FRCs). Lymph flow along the conduits delivers small molecular weight (MW; MW < 70 kDa) antigens to the T cell zone or the B cell follicles for effective antigen recognition (28–30). Another important function of conduit-mediated lymph flow is to deliver regulatory factors, such as chemokines and cytokines, to HEVs, which contributes to immune cell homing to the LN (27). It is not clear whether lymph distribution throughout the LN can regulate neutrophil recruitment in the LN.

Skin infections often occur where the skin barrier is disrupted either by injury or by skin diseases (31, 32). Dermatitis is a common skin disease, where dry and itchy skin cracks easily, making it prone to infection (33). In clinical settings, MRSA infection is hard to treat in dermatitis and causes a significant economic and health care burden (34). The persistent infection increases the risk of systemic bacterial dissemination (35, 36). Understanding the factors that regulate neutrophil migration to the LN during MRSA infection in dermatitis would help develop proper targets to promote host immune protection. Oxazolone (OX) skin contact sensitization induces skin inflammation (OX skin inflammation) and is often used to model contact and atopic dermatitis (37, 38). OX skin inflammation induces LN cell expansion, where the LN stromal cells and conduits undergo substantial remodeling (39, 40). Moreover, lymphatic vessel contraction and lymph flow to the LNs are reduced during OX skin inflammation (41, 42). It is, however, still unclear whether lymphatic dysfunction during OX skin inflammation impacts neutrophil migration in *S. aureus* skin infection.

In this study, we investigated how skin infection can effectively recruit neutrophils to the LN at the earliest time postinfection. By surgically suturing the afferent lymphatic vessels, we blocked lymph flow from the skin to the LN and prevented neutrophil recruitment to the LN at 4 hpi. However, within 4 hpi, the lymphatic vessels did not transport neutrophils from the skin to the LN but could effectively send *S. aureus* and soluble regulatory factors to the LN. Direct injection of *S. aureus* into the LN could not effectively recruit neutrophils to the LN. Instead, chemokine(C-X-C motif) ligand 1 (CXCL1) and CXCL2 injected in the skin were sufficient to recruit neutrophils to the LN. Therefore, lymph-borne chemokines were essential factors to activate HEVs to recruit neutrophils at the acute phase. During OX skin inflammation, lymphatic dysfunction not only reduced CXCL1/2 in the LN but also, reduced lymph (and its contents) reaching HEVs via the conduits. The compromised lymph flow was associated with impaired neutrophil interaction with *S. aureus*, allowing for persistent infection in the LN.

Results

The First Wave of Neutrophil Infiltration in the LN after *S. aureus* Infection Is Dependent on Functional Afferent Lymphatic Vessels. Within 4 h post–*S. aureus* infection (4 hpi), a large number of neutrophils are recruited to the LN (7–10). Neutrophils can infiltrate the LN from HEVs and lymphatic vessels after infection (7–14). Previous studies have established that neutrophils are not detected in the lymphatic vessels before 4 hpi (7). At 8hpi, approximately 2.5% neutrophils in the LN are trafficking from lymphatic vessels (11). Therefore, we expect more than 97% of the neutrophils to enter the LN via HEVs in the acute phase of neutrophil recruitment. We sought to investigate how skin infection communicates with the LN to efficiently recruit neutrophils via HEVs before 4 hpi.

Because lymph flow can report changes in the site of infection to the LN in a matter of minutes, we first investigated if functional lymphatic vessels contribute to neutrophil recruitment to the LN by 4 hpi. We used Evans Blue dye to visualize lymphatic vessels and surgically sutured afferent lymphatic vessels from the footpad to the popliteal lymph node (pLN) (Fig. 1*A*) (43). Using Flourescein isothiocyanate (FITC, ∼400 Da) as a tracer, lymph (indicated by FITC) could not effectively enter the LN nor reach HEVs, indicating that lymph flow from the skin to

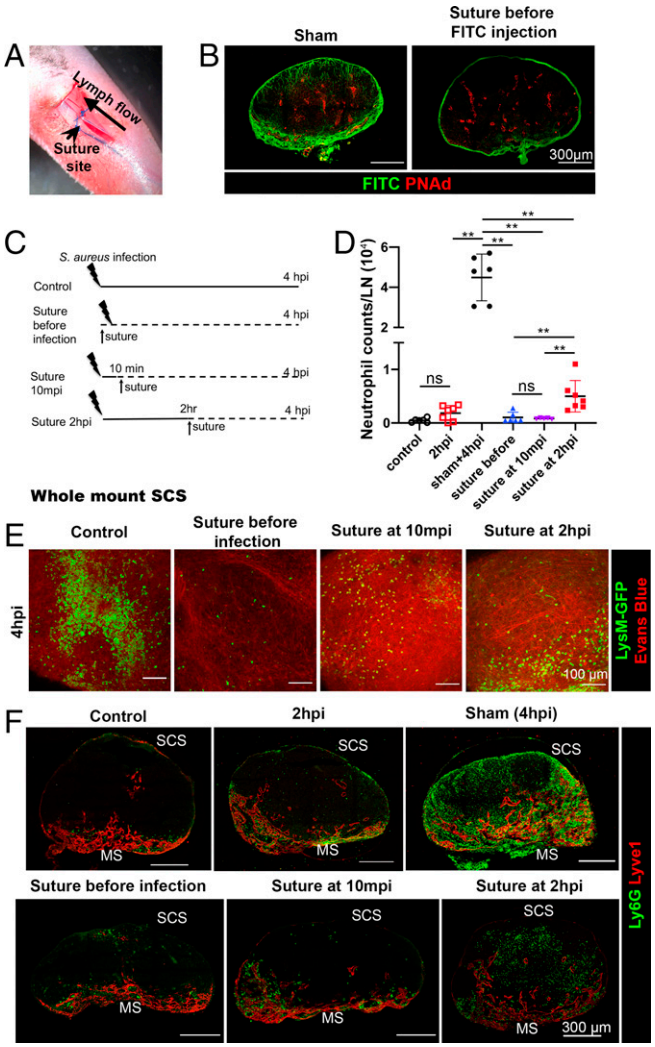

Fig. 1. The first wave of neutrophil recruitment in the LN depends on lymph flow. (*A*) A representative picture of the procedure of suturing afferent lymphatic vessels. (*B*) FITC distribution in pLN cryosections of sham and sutured WT mice after they are i.d. injected with FITC at the footpad. $n = 5$ per group. (*C*) Schematic diagram of lymphatic suture before infection, 10 mpi, and 2 hpi. (*D*) Neutrophils (CD11b$^+$Ly6G$^+$) in the draining pLN were quantified by flow cytometry. $n = 6$ to 7. Data are mean ± SD (Mann–Whitney test). (*E*) Neutrophil (LysM-GFP$^+$) accumulation on SCS by imaging whole-mount pLNs. $n = 3$ to 5 per group. (*F*) Cryosections of pLNs were stained with anti-Ly6G (green; neutrophils) and anti-Lyve1 (red; lymphatic endothelial cells). $n = 4$ to 5 per group. $^{**}P < 0.01$; ns, no significance.

the LN was blocked (Fig. 1*B*). Next, we sutured lymphatic vessels under three conditions: 1) before infection, 2) 10 min post-infection (mpi), and 3) 2 hpi. Skin incision with Evans Blue dye injection and *S. aureus* injection were performed as the sham group. All the LNs were collected at 4 hpi (Fig. 1*C*). The naïve LNs and LNs at 2 hpi were collected as negative and early time point controls, respectively. Using wild type (WT, C57BL/6J) mice to quantify the number of neutrophils ($CD11b^+Ly6G^+$) via flow cytometry, we found that neutrophils were recruited into the pLNs by 2 hpi and that the number sharply increased between 2 and 4 hpi. This recruitment was disrupted when lymphatic vessels were sutured before infection or at 10 mpi. When sutured at 2 hpi, there were more neutrophils in the pLNs compared with the first two time points, but there remained significantly fewer than those in the sham 4 hpi (Fig. 1*D*). Using the LysM-green fluorescent protein (GFP) reporter mice to trace neutrophils, we imaged the SCS of whole-mount pLNs and found neutrophil accumulation in the SCS at 4 hpi in control mice. When lymphatic vessels were sutured before the infection, at 10 mpi, or at 2 hpi, the number of neutrophils in the SCS was substantially fewer than those in the control pLNs at 4 hpi (Fig. 1*E*). WT mice LN cryosections also showed an increase of neutrophils in the LN at 2 hpi and a sharp increase from 2 to 4 hpi. At 2 hpi, most early arrival neutrophils were located in the MS, where Lyve1 staining was concentrated (Fig. 1*F*). Since neutrophils had been recruited to the LN before 2 hpi (the early time point control), more neutrophils were accumulated in the pLNs sutured at 2 hpi than those sutured before infection or at 10 mpi, but there were still significantly fewer than those in the sham pLN at 4 hpi (Fig. 1*F*). Thus, blocking lymphatic vessels either before or after infection significantly reduced neutrophil recruitment to the LN at 4 hpi.

In addition to carrying materials in and out of the LN, lymph flow plays a vital role in maintaining the homeostatic function of HEVs and cell compartmentalization in LNs (44–46). It is important to exclude the possibility that surgical intervention on lymphatic vessels impaired HEV and LN microenvironments, disrupting immune cell homing to the LN. Therefore, we adoptively transferred Carboxyfluorescein succinimidyl ester (CFSE)-labeled splenocytes to sham and sutured mice and collected the pLNs 4 h later (*SI Appendix*, Fig. 1*A*). Cryosections with immunofluorescence (IF) staining showed that $CFSE^+$ cell homing and distribution in the pLN were comparable between sham and sutured mice (*SI Appendix*, Fig. 1*B*). Flow cytometry analysis showed that the proportion and the number of $CFSE^+$ splenocytes in the LN as well as the composition of $CFSE^+$ cells (proportions of T cells, B cell, and myeloid cells) were comparable between sham and sutured mice (*SI Appendix*, Fig. 1 *C* and *D*). These results showed that HEV and the LN microenvironment for immune cell homing were intact at 4 h postsurgery, which was the time frame we focused on in this study.

Neutrophil Trafficking in Afferent Lymphatic Vessels Was Not Detected before 4 hpi. Next, we set out to investigate the mechanism by which blocking lymphatic vessels could prevent neutrophil migration to the LN. Because neutrophils can travel through lymphatic vessels to the draining LNs (11–13), we performed intravital time-lapse imaging of neutrophil migration in the footpad (injection site), the LN, and the afferent lymphatic vessels between 2 and 4 hpi. At 2 hpi, some neutrophils had entered the MS, few had moved to the SCS of the pLNs, and some neutrophils had entered the footpad. Between 2 and 4 hpi, neutrophils in the SCS and MS were sharply increased in the pLNs and the footpad. However, while we observed active neutrophil circulation in the blood vessels in the adipose tissue surrounding the afferent lymphatic vessels, we did not observe neutrophil trafficking in the afferent lymphatic vessels (Movie S1 and *SI Appendix*, Fig. 2). Since neutrophil trafficking in lymphatic vessels was below the detection level at 2 to 4 hpi and a substantial number of neutrophils had been recruited to the LN at 4 hpi, neutrophil lymphatic trafficking was unlikely to contribute to neutrophil recruitment via HEVs.

Without Lymph Flow or Skin Infection, Bacteria Alone in the LNs Are Not Effective in Recruiting Neutrophils. Next, we determined if lymph-borne bacteria trafficked to the LN were responsible for activating LN-resident cells (i.e., SCS macrophages) and recruiting neutrophils. *S. aureus* had entered the pLNs as early as 10 mpi, and the number of bacteria in the pLNs reached a plateau by 2 hpi by counting colony forming units (CFUs) in the LN (Fig. 2*A*). We sutured lymphatic vessels before infection, at 10 mpi, or at 2 hpi and collected the LNs at 4 hpi. As expected, when lymphatic vessels were sutured before infection, *S. aureus* could not enter the LN. *S. aureus* had already entered the pLNs when lymphatic vessels were sutured at 10 mpi and 2 hpi (Fig. 2*B*). In a separate experiment imaging the SCS of whole-mount LNs from mice infected with GFP-labeled *S. aureus,* the bacteria were in the SCS of both sham and sutured at 10 mpi groups but not in the sutured before infection group (Fig. 2*C*). Thus, *S. aureus* was able to enter the LN as early as 10 mpi. However, when lymphatic vessels were blocked, the presence of *S. aureus* in the LN was ineffective at recruiting neutrophils at 4 hpi (Fig. 1 *C*–*F*).

To further determine if the presence of bacteria in the LN without a concurrent skin infection could attract neutrophils, we intranodally (i.n.) microinjected 10^5 *S. aureus* with Evans Blue dye (Fig. 2*D*). Because pLNs were too small for i.n. injection, we performed this experiment in the inguinal lymph nodes (iLNs). PBS or *S. aureus* (with Evans Blue) intradermal (i.d.) infection at the flank served as a control. At 4 hpi, by imaging the SCS of whole-mount LNs and LN sections, i.d. infection at the flank showed substantial neutrophil accumulation in the SCS and throughout the LNs at 4 hpi (Fig. 2 *D*–*F*). However, only a small number of neutrophils were observed around the injection site in both PBS and *S. aureus* i.n. injection (indicated by Evens Blue dye) (Fig. 2 *D*, arrows, *E*, and *F*). The CFUs of *S. aureus* in the iLNs at 4 hpi were comparable between i.n. injection and i.d. infection (Fig. 2*G*). These results showed that without concurrent skin infection, the presence of *S. aureus* in the LN could not effectively recruit neutrophils to the LNs at 4 hpi either.

CXCL1 and CXCL2 in the Skin Are Sufficient to Recruit Neutrophils to the LN. Neutrophil recruitment through HEVs requires interaction with adhesion molecules (peripheral node addressin [PNAd]), integrins, and chemokines (7, 10). PNAd and integrins are conservatively expressed on HEVs for immune cell homing. Multiplex chemokine and cytokine discovery array analysis (31-plex; Eve Technology) showed that chemokines related to neutrophil recruitment, such as CXCL1 and CXCL2, had increased slightly in the pLN at 2 hpi, followed by a significant increase between 2 and 4 hpi (Fig. 2*H* and *SI Appendix*, Table 1). To determine if blocking lymph flow impaired CXCL1 and CXCL2 levels in the LN, we sutured the lymphatic vessels before infection or at 2 hpi (to give sufficient time for bacteria entry and LN-resident cell activation). Suturing either before infection or at 2 hpi resulted in lower

Fig. 2. Chemokines but not bacteria in the LN are essential to recruit neutrophils within 4 hpi. (*A*) Kinetics of *S. aureus* accumulation (CFUs) in pLNs (10 mpi, 2 hpi, and 4 hpi). (*B*) *S. aureus* CFUs in the pLNs at 4 hpi in control, suture before infection, and suture at 10 mpi groups. (*C*) GFP *S. aureus* distribution in the SCS by imaging whole-mount LN. $n = 3$ to 5 per group. (*D*) Neutrophil accumulation in iLNs at 4 hpi with i.d. or i.n. injection of Evans Blue or *S. aureus* plus Evans Blue in phosphate buffered saline (PBS). Evans Blue showed lymph distribution. Arrows indicate i.n. injection site. (*E* and *F*) Image quantification of neutrophils on SCS of whole-mount LN (*E*) and LN cryosection (*F*). (*G*) *S. aureus* CFUs in the LNs at 4 hpi with i.d. or i.n. *S. aureus* infection. (*H*) Chemokine/cytokine array of pLNs from control, 2 hpi, 4 hpi, suture before, and suture at 2 hpi groups. $n = 3$ to 4. (*I*) Chemokine/cytokine array of the pLN at 4 hpi in mice treated with rat IgG or anti-Gr1 antibody. $n = 4$. (*J*) Neutrophil (green) distribution in pLN at 2 h after rCXCL1, rCXCL2, or combination injection. $n = 5$ to 7. (*A*, *B*, and *E*–*J*). Data are mean ± SD (unpaired one-way ANOVA [*E*–*H* and *J*] or unpaired Student's *t* test [*I*]). $^{*}P < 0.05$; $^{**}P < 0.01$; $^{***}P < 0.001$; $^{****}P < 0.0005$; ns, no significance.

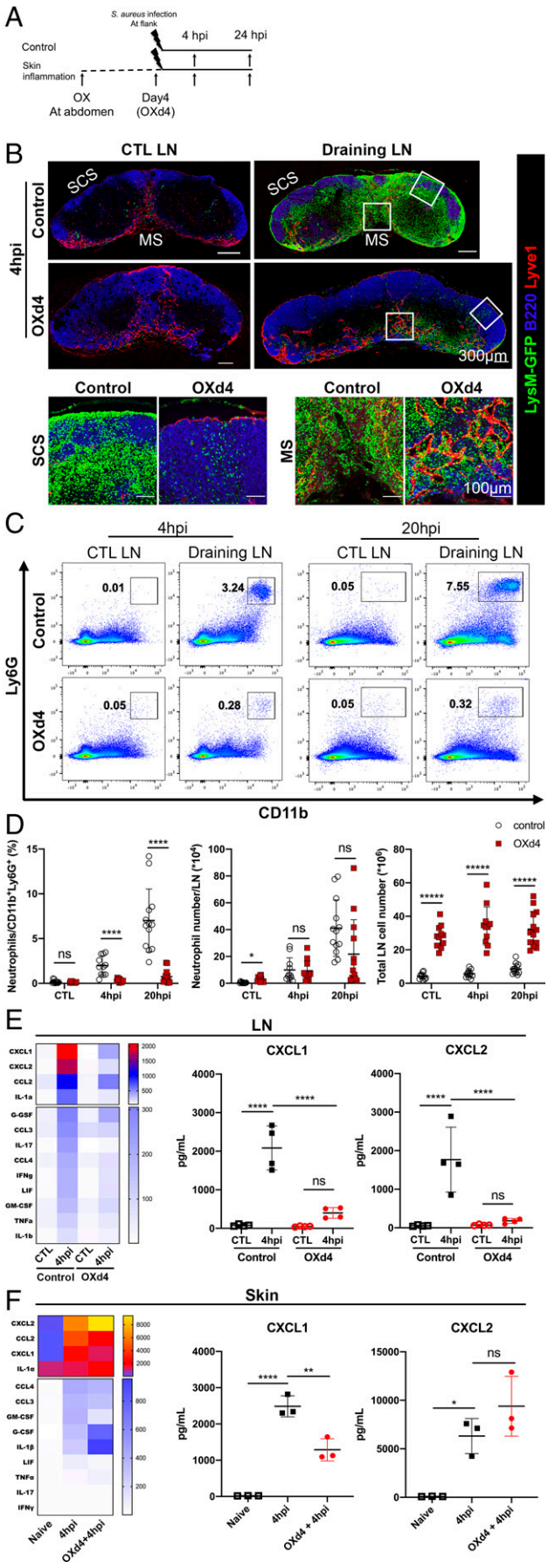

Fig. 3. OX skin inflammation interrupts neutrophil positioning when exposed to secondary infection. (*A*) The schematic diagram of the experimental design. Mice were treated with OX on their shaved abdomens. Four days after OX treatment (OXd4), control (uninflamed) and OXd4 (inflamed) mice were infected with 2.5×10^7 *S. aureus* i.d. in the right flank. The contralateral (CTL) and the draining iLNs were collected at 4 or 24 hpi. (*B*) Neutrophil distribution (LysM-GFP$^+$) at 4 hpi in iLN cryosections stained with anti-B220 (blue; B cells) and anti-Lyve1 (red). $n = 5$. (*C*) Representative flow cytometry scatterplots of neutrophil (CD11b$^+$Ly6G$^+$) at 4 and 20 hpi in control and OXd4 iLNs. (*D*) LN cell counts and neutrophil quantification at 4 and 20 hpi in control and OXd4 iLNs by flow cytometry. $n = 7$ to 9. Data are mean ± SD (multiple Student's *t* test). (*E* and *F*) Chemokine/cytokine level in the LN (*E*) and skin (*F*) of control and OXd4 mice. $n = 3$ to 4 per group. Data are mean ± SD (unpaired one-way ANOVA). $^*P < 0.05$; $^{**}P < 0.01$; $^{***}P < 0.001$; $^{****}P < 0.0005$; ns, no significance.

CXCL1 and CXCL2 levels in the LN (Fig. 2*H* and *SI Appendix*, Table 1). Considering that bacteria in the LN had reached a plateau by 2 hpi and that some neutrophils had already entered the LN (Figs. 1 and 2 *A*–*C*), these results showed that without active lymph flow, cells in the LN could not efficiently produce CXCL1 and CXCL2 at 4 hpi. Chemokines had also increased at 2 hpi and sharply increased between 2 and 4 hpi in the footpad. Blocking lymph flow did not impact CXCL1 and CXCL2 production in the footpad (*SI Appendix*, Fig. 3 and Table 2).

Although we could not exclude the possibility that LN-resident cells may require active lymph flow to maintain their chemokine production ability, these results indicated that CXCL1 and CXCL2 in the LN might come from the site of infection in skin with lymph flow. Therefore, we injected recombinant mouse CXCL1 (rCXCL1), rCXCL2, or both in the footpad. The draining pLNs were collected 2 h later, and the contralateral pLNs were collected as controls. Very few neutrophils were observed in control pLNs. Neutrophils were recruited to the draining pLNs in all these conditions (Fig. 2*J*). These results showed that lymph-borne proinflammatory chemokines from the skin were sufficient to recruit neutrophils in the LN as early as 2 h.

It is possible that the first wave of neutrophils in the LN at 2 hpi produces chemokines to recruit more neutrophils. Therefore, we depleted neutrophils by intraperitoneal injection of anti-Gr1 antibody or rat Immunoglobulin G (IgG) control 24 h prior to infection. The pLNs were collected at 4 hpi. CXCL1 concentration was comparable between control IgG and anti-Gr1 treated pLNs. CXCL2 levels were reduced in the anti-Gr1–treated mice (Fig. 2*I* and *SI Appendix*, Table 3) but remained substantially higher than control or sutured groups (*SI Appendix*, Tables 1 and 3). Thus, the first wave of neutrophils did not play a substantial role in chemokine production in the LNs. Together, these results showed that lymph-borne chemokines CXCL1/2 from skin were sufficient to recruit neutrophil to the LN via HEVs. Neither neutrophil trafficking in lymphatic vessels nor lymph-borne bacteria were essential contributors to neutrophil recruitment to the LN at 4 hpi.

Skin Inflammation Interrupts Neutrophil Recruitment in Response to *S. aureus* Infection. Inflammation is often associated with lymphatic dysfunction, such as suppressed lymphatic pumping and reduced lymph flow (41, 42, 47). To study if inflammation-induced lymphatic dysfunction alters neutrophil response upon infection, we used OX contact sensitization to induce skin inflammation that peaks at day 4 (OXd4). To avoid the interruption of cytokine and chemokine production at the infection site due to skin inflammation, we sensitized the mice with OX on the abdomen and injected *S. aureus* in the intact skin on the flank. iLNs were collected at 4 hpi (Fig. 3*A*). Only a few neutrophils were observed in the contralateral LN at OXd4 without infection (Fig. 3*B*, CTL). Neutrophils distributed throughout the draining iLNs at 4hpi, reaching both

the SCS and MS (Fig. 3*B*, top draining LN). In the OXd4 draining iLNs, the number of neutrophils appeared to be substantially reduced, and they were preferentially positioned in the MS (Fig. 3*B*, bottom draining LN). In order to determine if neutrophil recruitment or positioning in OXd4 LNs can be restored given a longer time point, we collected the control and OXd4 iLNs at 24 hpi. By this time, neutrophils had migrated away from the SCS of control draining LNs. However, in the OXd4 draining iLNs, the neutrophils remained restricted in the MS, which indicates they could not migrate to the SCS, even at a later time point (*SI Appendix*, Fig. 4). Because LNs had substantially expanded at OXd4, we further quantified the absolute number of neutrophils in the LNs by flow cytometry. While the proportion of neutrophils in OXd4 iLNs was significantly reduced, the number of neutrophils per LN was not significantly different compared with the control LNs at 4 or 20 hpi (Fig. 3 *C* and *D*). Therefore, the proportion and the positioning of neutrophils, rather than the number of neutrophils, were substantially changed after *S. aureus* infection in OXd4 iLNs.

Because lymph-borne chemokines are the major contributors to the neutrophil recruitment in the LN, we measured the concentration of proinflammatory chemokines in the LN by multiplex chemokine and cytokine discovery array. Without infection, CXCL1 and CXCL2 levels were low and comparable between control and OXd4 iLNs. CXCL1 and CXCL2 were increased but significantly lower in the OXd4 4 hpi iLNs than control 4 hpi iLNs (Fig. 3*E* and *SI Appendix*, Table 4). CXCL1 in the skin infection site of OXd4 mice was reduced but remained significantly higher than the controls. CXCL2 in skin infection sites was comparable between control and OXd4 infections (Fig. 3*F* and *SI Appendix*, Table 5). These data demonstrated that OXd4 LNs were unable to effectively recruit neutrophils from the HEVs in response to *S. aureus* skin infection.

Neutrophil Positioning in the SCS Is Not Dependent on SCS Macrophages. To better understand the molecular mechanism of how OX skin inflammation changed neutrophil recruitment in OXd4 iLNs, we collected control and OXd4 iLNs at 4 hpi to compare their proteomes (*SI Appendix*, Fig. 5*A*). Based on the Reactome Pathway analysis (using STRING v11.0 [https://string-db.org]) of the enriched proteins in LNs at 4 hpi, CD169 expression was significantly reduced in OXd4 LNs (Fig. 4*A*). To verify the proteomic analysis results, the reduction of CD169 expression in the SCS was demonstrated by cryosections with IF staining (Fig. 4*B*), and the median fluorescent intensity (MFI) was marginally reduced by flow cytometry analysis (Fig. 4*C*). Whole-mount imaging of the SCS showed a significant reduction of CD169$^+$ macrophages in OXd4 iLNs (Fig. 4*D*). Together, these results verified the reduced CD169 expression in OXd4 LNs identified by the unbiased proteomic analysis.

CD169$^+$ SCS macrophages are the first layer of cells in the LN that encounter microbes trafficked via afferent lymphatic vessels, and they play a critical role in bacterial phagocytosis and production of proinflammatory cytokines to recruit other types of cells (5). To determine if the reduced CD169$^+$ macrophage layer impaired neutrophil migration, we used clodronate liposomes to deplete macrophages in the pLNs and PBS liposomes as controls. Depletion of CD169$^+$ macrophages was confirmed by IF staining (Fig. 4*E*). At 4 hpi, there was no difference in neutrophil recruitment or positioning in the SCS (Fig. 4*E*). Therefore, neutrophil migration was not dependent on the CD169$^+$ SCS macrophages after *S. aureus* infection, which is consistent with a previous report (7).

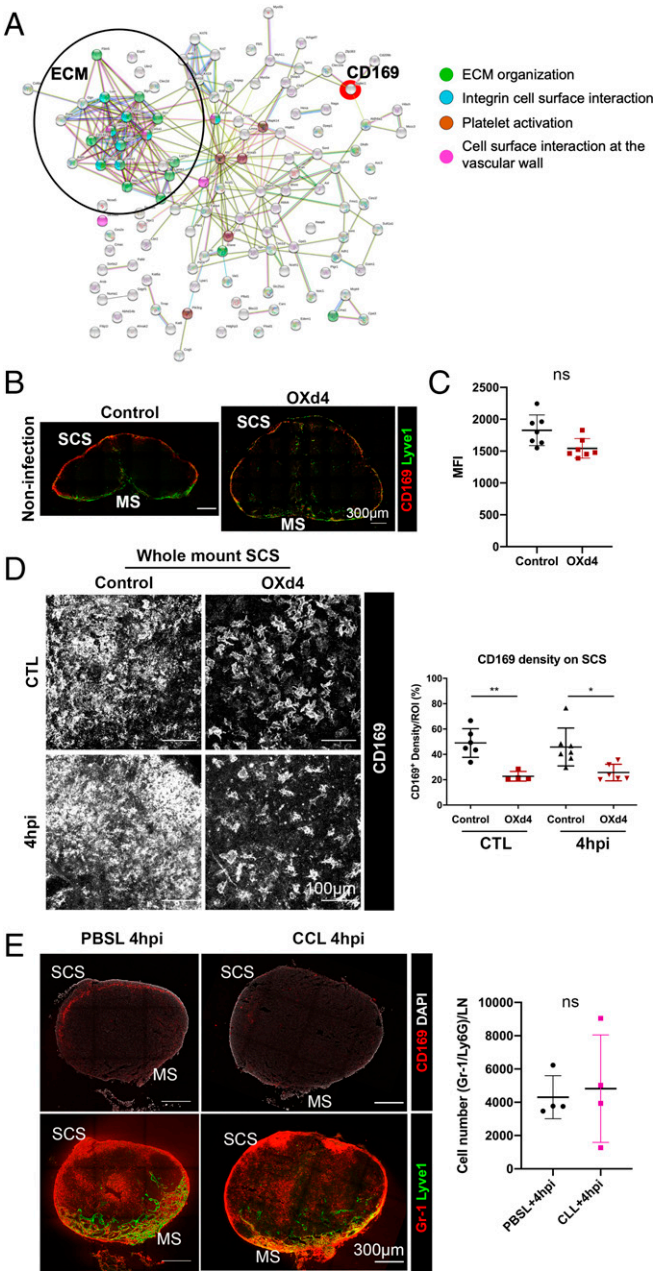

Fig. 4. Neutrophil migration does not depend on SCS macrophages. (*A*) Proteomics analysis. LNs were collected from control and OXd4 mice at 4 hpi. Reactome pathway analysis using STRING-DB showed reduced ECM proteins and Siglec1 (CD169) in the OXd4 LNs compared with the control LNs. (*B*) CD169 (red) and Lyve1 (green) in control and OXd4 LNs. (*C*) MFIs of CD169 in control and OXd4 LNs quantified by flow cytometry. (*D*) Anti-CD169 IF staining on whole-mount iLNs collected at 4 hpi (gray; SCS macrophages; *Left*). CD169 density on SCS quantification per region of interest (ROI; *Right*). $n = 7$. (*E*) Neutrophil recruitment in macrophage depletion mice. (*Upper Left*) Anti-CD169 (red) and DAPI (gray; nuclei staining). (*Lower Left*) Anti-Lyve1 (green) and anti-Gr1 (red; neutrophils and monocytes). $n = 4$ per group. (*C*–*E*) Data are mean ± SD (unpaired Student's *t* test). CLL, clodronate liposome; PBSL, PBS liposome. $^*P < 0.05$; $^{**}P < 0.01$; ns, no significance.

LN Remodeling Impairs Lymph Flow along the Conduits but Not around the Sinus. Based on the Reactome Pathway analysis, we also identified a network of ECM proteins, including collagens I, II, IV, and VI as well as Laminin 1 and Laminin 2, that were reduced in OXd4 LNs (Fig. 4*A*). ECM proteins are major components of LN conduits, which facilitate lymph flow and trafficking of small MW material from the SCS to the T cell zone and HEVs. LN cryosections showed that the

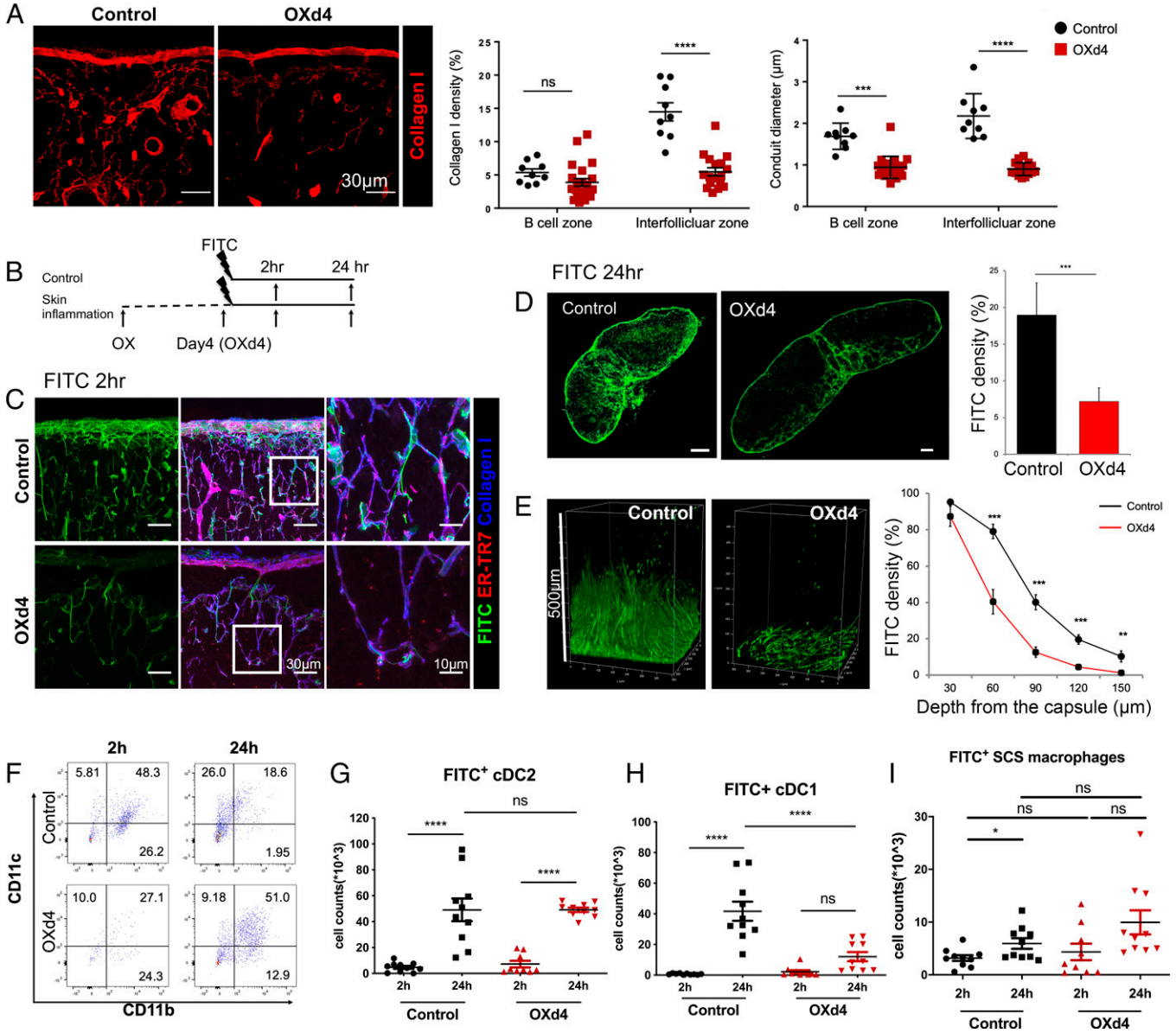

Fig. 5. OX skin inflammation impairs lymph flow in conduits. (*A*) Conduit (red) in control and OXd4 iLNs (*Left*). The density (*Center*) and the diameter (*Right*) of collagen I$^+$ conduits in the iLNs of control and OXd4 mice. $n = 4$ to 5 per group. (*B*) The schematic diagram of the experimental design. Mice were treated with OX on their shaved abdomens. The control and OXd4 mice were treated with FITC on both flanks. After 2 or 24 h, the iLNs were collected for analysis. (*C*) FITC distribution with conduits in the iLNs at 2 h after FITC sensitization. LN cryosections were stained with anti-ERTR7 (red; FRCs) and anti-collagen I (blue; conduit). (*D*) FITC distribution (*Left*) and density (*Right*) at 24 h after FITC sensitization. Scale bar = 200 μm. (*E*) 3D-reconstructed images of FITC in whole-mount LN at 24 h after FITC sensitization (*Left*). FITC density with depth was quantified every 30 μm from the capsule (*Right*). $n > 5$ mice per group. (*F–I*). Control and OXd4 LNs were collected at 2 and 24 h after FITC sensitization. (*F*) Representative flow cytometry plot of FITC$^+$ DCs. (*G–I*) FITC$^+$cDC2, cDC1, and SCS macrophage quantification. $n = 10$ iLNs/group. (*A*, *D*, *E*, and *G–I*) Data are mean ± SEM (unpaired one-way ANOVA [*A* and *G–I*] or unpaired Student's *t* test [*D* and *E*]). *$P < 0.05$; **$P < 0.01$; ***$P < 0.001$; ****$P < 0.0005$; ns, no significance.

density and diameter of collagen I$^+$ conduits were significantly reduced in OXd4 LNs compared with control LNs (Fig. 5*A* and *SI Appendix*, Fig. 6). To understand if the reduced conduit density and diameter impact lymph flow in the LN, control and OXd4 LNs were collected 2 or 24 h after FITC treatment (Fig. 5*B*). Much less FITC was detected in LN conduits of OXd4 LNs compared with control LNs (Fig. 5*C*). At 24 h post-FITC treatment, FITC was still restricted to the SCS and MS in OXd4 LNs compared with control LNs (Fig. 5*D*). After optical clearing with Benzyl Alcohol/ Benzyl Benzoate (BABB), three-dimensionally (3D) reconstructed images showed that FITC could not penetrate OXd4 LNs as deep as control LNs (Fig. 5 *E*, *Left*). Quantification of FITC density was performed every 30 μm from the LN SCS inward, revealed that FITC density was comparable between control and OXd4 LNs in the first 30 μm from the capsule, but FITC density was substantially reduced in OXd4 LNs for the subsequent 30 to 150 μm from the capsule (Fig. 5 *E*, *Right*). To rule out the potential impacts on FITC distribution by sample processing, we used time-lapse intravital live imaging to track FITC distribution in LNs. Consistently, FITC entered the conduits and penetrated deep into control LNs (Movie S2). In OXd4 LNs, FITC was restricted to the sinus (Movie S3). Together, these results showed that OX inflammation reduced conduits and impeded lymph penetration into the LN parenchyma via conduits but did not significantly reduce lymph flow from the SCS to MS.

To further verify if the altered lymph flow distribution impacted immune cell activation in the LN, we measured LN-resident DC

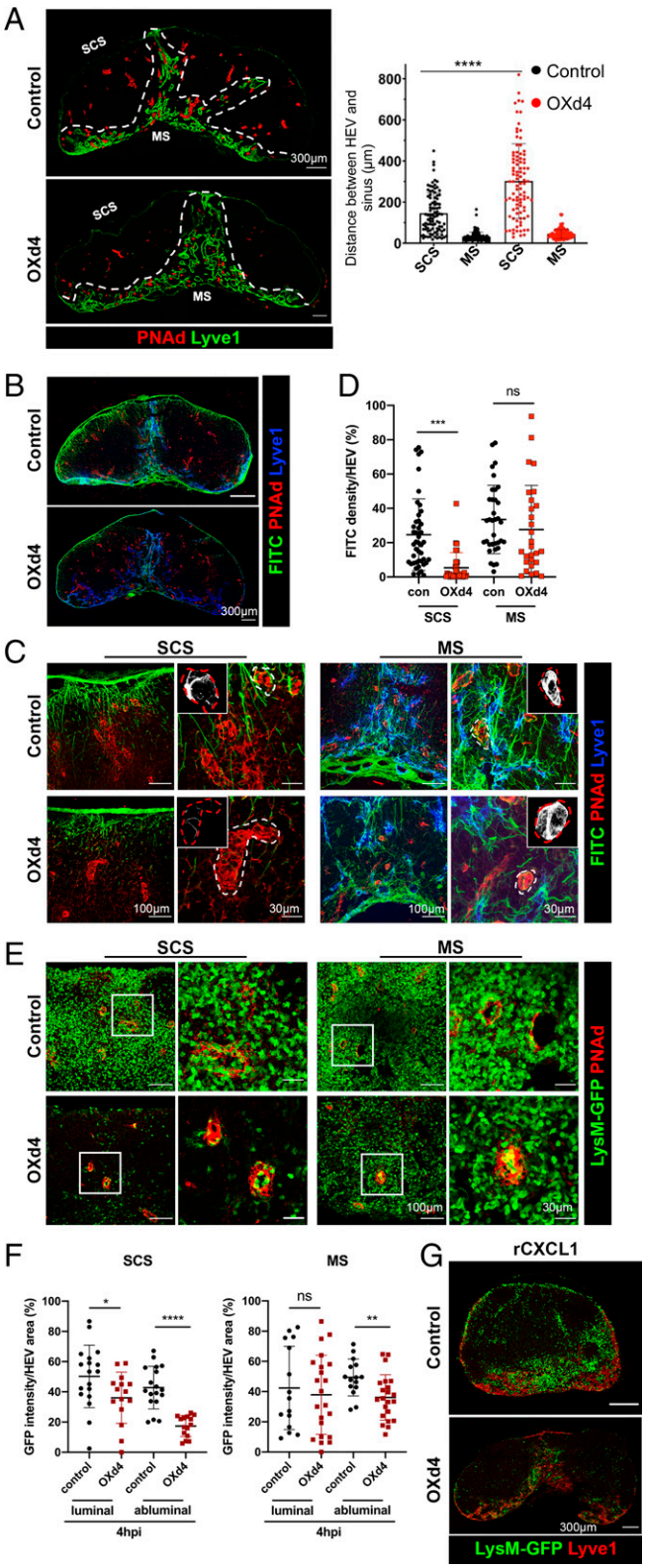

Fig. 6. OX skin inflammation interrupts lymph reaching HEVs and changes neutrophil migration in HEVs. (*A*) Distribution of HEVs in control and OXd4 iLNs. Cryosections were stained with anti-PNAd (red; HEV) and anti-Lyve1 (green) antibodies to show HEVs and sinuses (*Left*). The distance between HEVs with the SCS or MS in the control and OXd4 LNs (*Right*). $n = 4$. (*B* and *C*) FITC HEV distribution in control and OXd4 iLNs at 4 h after FITC treatment. (*D*) Quantification of FITC density per HEV near the SCS or MS in control and OXd4 iLNs. $n = 5$ to 6. Data are mean ± SD (unpaired Student's *t* test). (*E*) Neutrophil (LysM-GFP) distribution around HEVs (PNAd) in control and OXd4 LN. (*F*) Neutrophil (GFP) intensity in luminal and abluminal areas of HEVs (PNAd). $n = 4$ to 5. Data are mean ± SD (unpaired Student's *t* test). (*G*) Neutrophil (LysM-GFP) distribution in the pLNs 2 h after rCXCL1 injection. $n = 4$. $^*P < 0.05$; $^{**}P < 0.01$; $^{***}P < 0.001$; $^{****}P < 0.0005$; ns, no significance.

activation by FITC. It is known that LN-resident DCs are divided into two major populations, cDC1 and cDC2. cDC1 ($CD11b^-CD11c^+$) is located deeper in the T cell zone, while cDC2 ($CD11b^+CD11c^+$) is located close to the SCS and MS (26). Flow cytometry results showed that the number of $FITC^+$ cDC1 (DCs that captured FITC) was substantially reduced in OXd4 LNs compared with control LNs, while the numbers of $FITC^+$ cDC2 and $FITC^+CD169^+$ SCS macrophages between control and OXd4 LNs at 2 and 24 h after FITC sensitization are comparable (Fig. 5 *F–I*). Together, these results showed that in the OXd4 LNs, lymph could flow around the SCS to the MS, but it could not effectively enter the T cell zone via conduits.

Inflammation Impairs Lymph from Reaching HEVs via Conduits but Not in the MS. HEVs are located deep in the T cell zones and in the MS of LNs (48–50). Chemokines in lymph can diffuse from the sinuses to the nearby HEVs or flow along the conduits to HEVs. Therefore, we examined how lymph can reach HEVs between control and OXd4 LNs. Using LN cryosections, we measured the distance from the SCS to the HEVs or from the MS to HEVs in the LNs. The results showed that OX skin inflammation substantially increased the distance from the SCS to HEVs but not from the MS to HEVs (Fig. 6*A*). Using FITC as a lymph tracer, in control LNs, a strong FITC signal was detected around HEVs near both the SCS and MS at 4 h post-FITC treatment (Fig. 6 *B-D*, control). In OXd4 LNs, FITC signal was restricted to the SCS and MS. Only a small amount of FITC from the SCS could reach HEVs located in the interfollicular or T cell zone (close to SCS). In the MS, despite a slightly weaker FITC signal, HEVs located near the MS remained exposed to FITC (Fig. 6 *B-D*, OXd4). These results suggested that due to the increased distance and reduced conduits in OXd4 LNs, lymph preferentially reached HEVs in the MS of OXd4 LNs. Thus, lymph-borne soluble factors (including chemokines) in OXd4 LNs were unable to diffuse or flow along the conduits to HEVs in the interfollicular or the T cell zones.

Neutrophils Preferentially Migrate via HEVs Located in the MS. We used LysM-GFP mice to characterize neutrophil transmigration in HEVs located in different areas of LNs. In control LNs, at 4 hpi, neutrophils were detected in both the luminal and abluminal sides of HEVs across the LN (Fig. 6 *E*, control and *F*, control). In OXd4 LNs, slightly fewer neutrophils were detected in the lumen of HEVs close to the SCS (interfollicular and the T cell zone). However, a substantially reduced neutrophil count on the abluminal side of HEVs indicated a significantly reduced neutrophil transmigration from HEVs to the OXd4 LN (Fig. 6 *E*, SCS and *F*, SCS). In the MS of OXd4 LNs, there was no significant difference between the number of neutrophils in the lumen of HEVs compared with control LNs. Neutrophils on the abluminal side of HEVs in OXd4 LNs were only slightly reduced compared with control LNs (Fig. 6 *E*, MS and *F*, MS).

To further determine whether altered lymph flow reduced lymph-borne chemokines to recruit neutrophils in the OXd4 LN, we injected rCXCL1 in the footpads of control and OXd4 mice (without infection) and collected their pLNs 2 h later. Neutrophil positioning in the OXd4 LNs was altered, preferentially located in the MS compared with control LNs (Fig. 6*G*).

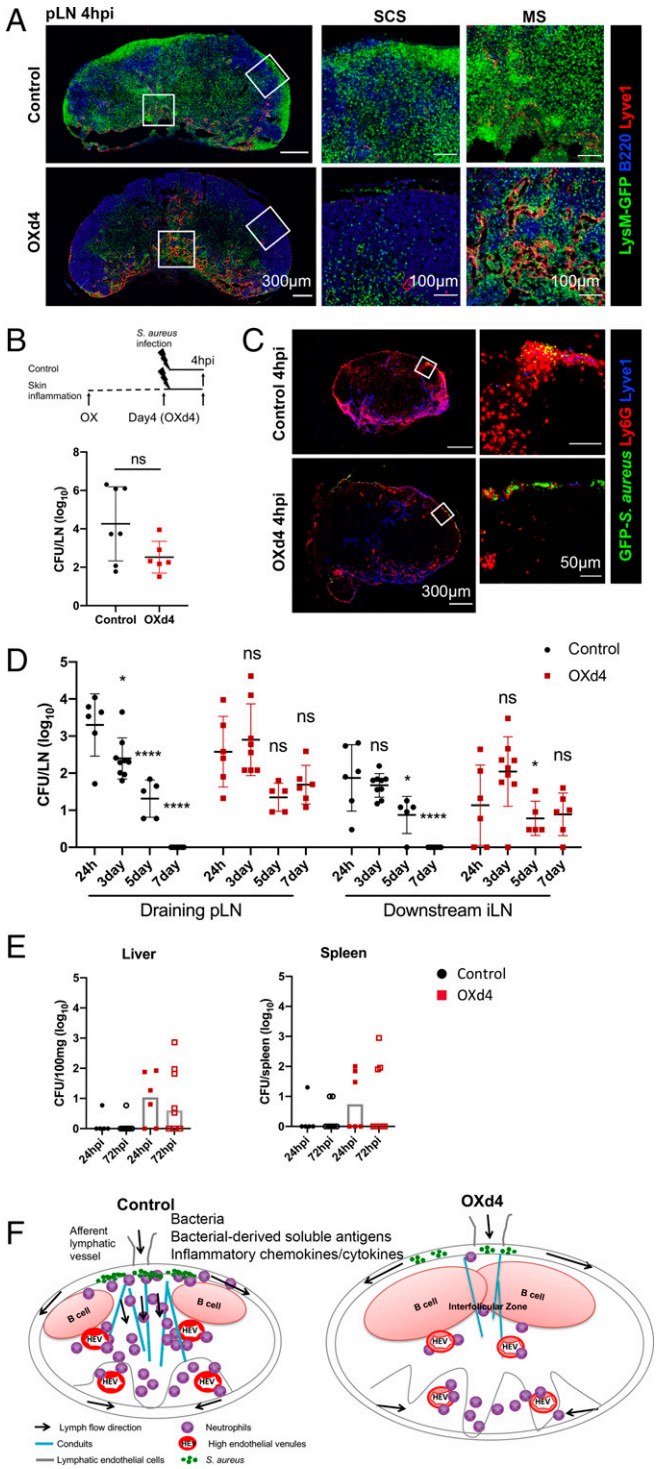

Fig. 7. Delayed bacterial clearance in the OXd4 LNs. (*A*) Neutrophil distribution (LysM-GFP) in pLNs at 4 hpi in control and OXd4 mice. (*B*) The schematic diagram of the experimental design (*Upper*). *S. aureus* was injected in the footpad of control and OXd4 mice. The draining pLNs were collected at 4 hpi. *S. aureus* CFUs (*Lower*) in control and OXd4 pLNs. $n = 6$ per group. Data are mean ± SD (unpaired Student's *t* test). (*C*) GFP *S. aureus* and neutrophil distribution in the control and OXd4 pLNs. (*D* and *E*) Bacterial load (CFUs) in control and OXd4 mice. The draining pLNs, downstream iLNs (*D*), spleen, and liver (*E*) were collected on different days postinfection. $n = 6$ to 8 per group. Data are mean ± SD (unpaired one-way ANOVA). (*F*) Schematic diagram of neutrophil positioning in the LN. At an early stage of infection, lymph flow transports *S. aureus* to the SCS. Soluble antigens and regulatory factors in lymph can reach the HEVs throughout the LN to direct neutrophils migration. Skin inflammation reduces the transport of lymph-borne factors (including chemokines) to the LN. LN cell expansion and conduit remodeling change lymph–HEV communication in LN. Lymph could reach HEVs in the MS but not those in the interfollicular and T cell zone (close to the SCS). Consequently, neutrophils preferentially transmigrate through the HEVs in the MS of the OXd4 LNs. $^{*}P < 0.05$; $^{****}P < 0.0005$; ns, no significance.

Collectively, concurrent with reduced lymph along the conduits in the OXd4 LN, neutrophils did not migrate in the HEVs close to the SCS. However, neutrophils were able to transmigrate via HEVs located in the MS, where HEVs remained exposed to lymph (including lymph-borne chemokines) in OXd4 LNs.

Bacterial Clearance Is Delayed in OXd4 LNs. *S. aureus* is restricted to the SCS of LNs after infection. Neutrophils play a critical role in phagocytosis, killing bacteria and preventing bacterial systemic dissemination. We investigated whether the interrupted neutrophil positioning to the SCS in OXd4 LNs had an impact on *S. aureus* clearance. In LysM-GFP reporter mice, neutrophils could not migrate to the SCS in OXd4 pLNs, a similar result to our observations in OXd4 iLNs (Fig. 7*A*). We collected control and OXd4 pLNs at 4 hpi and quantified the bacterial load by counting CFUs. The CFUs were not significantly different between control and OXd4 mice at 4 hpi, indicating that OX inflammation did not prevent bacteria entering the LNs (Fig. 7*B*). When using GFP *S. aureus* to observe bacteria distribution in the LN, we found that GFP *S. aureus* at 4 hpi was restricted to the SCS in both control and OXd4 LNs. Neutrophils were accumulated around the GFP *S. aureus* in control LNs but not in OXd4 LNs (Fig. 7*C*), confirming that neutrophils could not reach the SCS in OXd4 and left the *S. aureus* unattended.

Because neutrophils play important roles in killing bacteria in the LN, we quantified the number of bacteria at various time points postinfection to determine the duration of infection in the LNs and to determine how the impaired neutrophil positioning in the LN impacts bacteria clearance. In control pLNs, the bacterial load was substantially reduced from 24 hpi to 3 d postinfection (dpi) and was entirely cleared by 7 dpi. In OXd4 pLNs, the number of bacteria remained similar from 24 hpi to 7 dpi (Fig. 7*D*). To determine if bacteria spread to downstream LNs or into circulation, we collected the downstream iLNs, blood, liver, and spleens to count the CFUs. Bacteria could spread to downstream iLNs in both control and OXd4 mice by 24 hpi, and persistent infection was observed in the OXd4 iLNs but not in control iLNs (Fig. 7*D*). *S. aureus* was barely detected in the blood in either control or OXd4 mice (*SI Appendix*, Fig. 7). Systemic dissemination of *S. aureus* is dominantly sequestered in the liver and the spleen after 30 min (51). We observed a trend of increase of *S. aureus* spreading into the liver and spleen of OXd4 mice (Fig. 7*E*). Thus, impaired neutrophil positioning resulted in persistent infection in the LN and a trend of increased systemic spreading of infection during OX skin inflammation.

Discussion

Skin-draining LNs play a pivotal role in eliminating and preventing the systemic spread of pathogens during SSTIs. One critical early step is the rapid recruitment of neutrophils to the LNs, which can kill bacteria and prevent systemic dissemination (7, 9). By blocking lymph flow before or at a short time after *S. aureus* infection, our studies showed that rapid neutrophil recruitment to the LN via HEVs depends on functional lymphatic vessels. Lymphatic vessels transport cells, bacteria, and soluble factors (including bacterial-derived free-form antigens and infection-induced regulatory factors) from the skin to the LN. Lymph flow in the LN facilitates the distribution of

lymph-borne materials. We aimed to establish which components of lymph are essential for rapid neutrophil recruitment to the LN within 4 hpi. Skin-derived migrating antigen-presenting cells (DCs) will not arrive in the LN via lymphatic vessels by 4 hpi and thus, are unlikely to trigger the first wave of neutrophil recruitment via HEVs (17, 52). Previous studies have shown that neutrophils can travel through lymphatic vessels to the LN (11–13). We showed that while the neutrophil number sharply increased in both the footpad and the LNs between 2 and 4 hpi, lymphatic trafficking of neutrophils was not detectable between 2 and 4 hpi by time-lapse images. Bogoslowski et al. (7) also showed that blocking neutrophil HEV transmigration abrogated neutrophil recruitment to the LN, demonstrating that neutrophils were recruited via HEVs before 4 hpi. Although cells migrating from lymphatics are usually present in the SCS, it is important to note that neutrophils in the SCS do not solely come from lymphatic vessels. After a skin infection, neutrophils can migrate from HEV to SCS very quickly to interact with bacteria restricted in the SCS (7, 8). These observations proved that the first wave of neutrophils was recruited from HEV in LN. Even if there is a small number of neutrophils that migrate from lymphatic vessels, the neutrophil lymphatic trafficking did not contribute to the early neutrophil recruitment via HEVs.

Our results did not conflict with the fact that neutrophils can travel through lymphatic vessels to the LN at later times or in other conditions. Hampton et al. (11) performed photoconversion on the infected skin area at 4 hpi and collected LN at 8 hpi (4 to 8 hpi). During this time frame, around 2.5% of the neutrophils in the LNs came from lymphatic vessels (11). Studies by Rigby et al. (12) and Gorlino et al. (13) did not quantify the proportion of the neutrophils that came from lymphatic vessels or blood vessels. Rigby et al. (12) showed that the rapid neutrophil adhesion and transmigration across lymphatic endothelial cells only occurred when lymphatic endothelial cells were preactivated with tumor necrosis factor α (TNFα) for 24 h. Gorlino et al. (13) injected isolated neutrophils to better study the mechanism of neutrophil lymphatic trafficking. Thus, neutrophil lymphatic trafficking requires sufficient neutrophils in the skin and activated lymphatic vessels. Neutrophils usually do not reside in healthy skin. For spontaneous neutrophil lymphatic migration postinfection, neutrophils first need to exit from the bloodstream and enter the infected skin. Skin neutrophils may then invade the lymphatic vessels and travel to the LN. Time to activate lymphatic vessels for neutrophil migration would also be required. In physiological conditions, these steps might take a few hours. Therefore, 0 to 4 and 4 to 8 hpi are significantly different time frames for spontaneous neutrophil lymphatic trafficking. The differences in time, mechanism, and function between lymphatic trafficking neutrophils and HEV trafficking neutrophils require future comprehensive studies.

Even though our results showed that lymphatic vessels did not directly transport neutrophils to the LN by 4 hpi, they still delivered *S. aureus* and regulatory factors. We showed that chemokines (CXCL1 and CXCL2) in the skin were sufficient to recruit neutrophils in the LN as early as 2 h. While CXCL1/2 are trafficked in the lymph, they are not the only lymph-borne factors to reach the draining LN. Other regulatory factors, such as chemokine (C-C motif) ligand 2 (CCL2) and complement component 5a (C5a), can also flow to the LN. *S. aureus* is able to reach the LN and could be responsible for the recruitment of neutrophils in the LN by activating LN-resident immune cells to produce CXCL1 and CXCL2. Our study showed that *S. aureus* enters the LN as early as 10 mpi and reaches a plateau by 2 hpi. When lymphatic vessels were sutured at 2 hpi, there was sufficient *S. aureus* in the LN to activate LN-resident cells. However, CXCL1, CXCL2, and other inflammatory chemokines and cytokines were globally reduced in the LN. Additionally, i.n. injection of *S. aureus* could not effectively recruit neutrophils to the LN. These results together suggested that without lymph flow or the concomitant skin infection, the presence of bacteria in the LN could not effectively produce CXCL1 and CXCL2 nor recruit neutrophils by 4 hpi. Our study could not exclude the possibility that active lymph flow might be required to maintain the activity of LN-resident cells or that i.n. injected bacteria might not activate proper populations of LN-resident cells at 4 hpi. However, these possibilities do not conflict with the conclusion that neutrophil migration in the LN depends on active lymph flow from skin to the LN nor do they exclude the importance of LN-resident cell activation in other steps of immune protection or other types of infection in the LN (2, 19, 53).

Lymphatic dysfunction often occurs during inflammation (41, 42, 47). OX skin inflammation is used to study lymphatic dysfunction as well as dermatitis (37, 38). Our study showed that lymph could not effectively reach HEVs in OX-treated mice, especially in the interfollicular and T cell zones. The impaired lymph flow is associated with altered neutrophil response in OX-inflamed LNs. Neutrophils in LN are essential in clearing local bacteria and systemic spreading during *S. aureus* infection (7). We found delayed bacterial clearance and a trend of increased systemic dissemination in the OX inflammation model. Dermatitis increases the risk of SSTI, and persistent skin infection also increases the risk of bacterial systemic dissemination (bacteremia). Our findings suggested a potential mechanism of prolonged MRSA infection in dermatitis.

It has been reported that constant lymph flow is required to maintain HEV-specific gene expression and LN cell homeostasis (44, 46, 54, 55). HEV-specific gene expression is reduced in the LN during OX skin inflammation (45, 56–58). It is, therefore, possible that the altered lymph flow changes HEV-specific gene expression and hence, reduces neutrophil migration. However, the neutrophil–HEV luminal interaction and the total number of neutrophils at 4 hpi were comparable between control and OXd4 LNs, indicating the reduced HEV gene expression was not the major factor for the neutrophil positioning in the MS of the OXd4 LNs. OX skin inflammation induced global changes in the LN microenvironment. However, integrin-α_1, -α_M, -β_1, -β_2, and -α_L were comparable between control and OXd4 LNs (proteomic analysis), indicating that neutrophil surface integrins were not interrupted by skin inflammation. Additionally, we examined the number of circulating neutrophils and the chemokine receptors on circulating neutrophils at 4 hpi between control and OXd4 mice. The numbers of circulating neutrophils in blood at 4 hpi are similar between control and OXd4 mice. The L-selectin, CXCR2, CXCR4, and C5aR were also similar, indicating that OX inflammation did not significantly reduce circulating neutrophils or the availability of the molecules required for neutrophil recruitment to the LN (*SI Appendix*, Fig. 8). Changes in lymph distribution in the LN played a critical role in regulating neutrophil migration to the LNs in *S. aureus* infection during skin inflammation.

In summary, active lymph flow carries regulatory factors from the infected skin to the LN and facilitates the distribution of lymph components to proper locations to ensure spatial and temporal neutrophil recruitment from HEVs into the LN. During skin inflammation, interrupted lymph flow impaired neutrophil migration and was associated with persistent infection in the

LN and a trend of bacteremia when exposed to *S. aureus* infection (Fig. 7*F*).

Materials and Methods

All animal protocols were reviewed and approved by the University of Calgary Animal Care and Ethics Committee. C57BL/6 mice were infected with MRSA in healthy condition and during the OX-induced skin inflammation condition. Lymph drainage was blocked by surgical suture. Lymph drainage and neutrophil infiltration in the LN were studied at 4 hpi by fixed sample imaging, intravital time-lapse imaging, and flow cytometry analysis. More information is provided in *SI Appendix*.

Data Availability. All study data are included in the article and/or supporting information.

ACKNOWLEDGMENTS. We thank Dr. Paul Kubes and Ania Bogoslowski for their critical input into this study. This work is supported by the University of Calgary start-up fund (S.L.), the Kipnes Lymphatic Imaging Suite supported by the Dianne & Irving Kipnes Foundation, Natural Sciences and Engineering Research Council of Canada Grant 03641, Canadian Institute of Health Research Grant PJT-156035, and Canada Foundation for Innovation Grant 32930 (to S.L.).

Author affiliations: [a]Inflammation Research Network, Department of Microbiology, Immunology and Infectious diseases, Snyder Institute for Chronic Diseases, Cumming School of Medicine, University of Calgary, Calgary, AB, Canada T2N 4N1; [b]Department of General Surgery, The Second Affiliated Hospital of Harbin Medical University, Harbin Medical University, Harbin, Heilongjiang, 150086, China; and [c]Department of Physiology & Pharmacology, McCaig Institute for Bone and Joint Health, Cumming School of Medicine, University of Calgary, Calgary, AB, Canada T2N 4N1

1. E. Kolaczkowska, P. Kubes, Neutrophil recruitment and function in health and inflammation. *Nat. Rev. Immunol.* **13**, 159–175 (2013).
2. W. Kastenmüller, P. Torabi-Parizi, N. Subramanian, T. Lämmermann, R. N. Germain, A spatially-organized multicellular innate immune response in lymph nodes limits systemic pathogen spread. *Cell* **150**, 1235–1248 (2012).
3. M. Y. Gerner, P. Torabi-Parizi, R. N. Germain, Strategically localized dendritic cells promote rapid T cell responses to lymph-borne particulate antigens. *Immunity* **42**, 172–185 (2015).
4. S. Liao, P. Y. von der Weid, Lymphatic system: An active pathway for immune protection. *Semin. Cell Dev. Biol.* **38**, 83–89 (2015).
5. H. Qi, W. Kastenmüller, R. N. Germain, Spatiotemporal basis of innate and adaptive immunity in secondary lymphoid tissue. *Annu. Rev. Cell Dev. Biol.* **30**, 141–167 (2014).
6. T. Junt *et al.*, Subcapsular sinus macrophages in lymph nodes clear lymph-borne viruses and present them to antiviral B cells. *Nature* **450**, 110–114 (2007).
7. A. Bogoslowski, E. C. Butcher, P. Kubes, Neutrophils recruited through high endothelial venules of the lymph nodes via PNAd intercept disseminating *Staphylococcus aureus*. *Proc. Natl. Acad. Sci. U.S.A.* **115**, 2449–2454 (2018).
8. O. Kamenyeva *et al.*, Neutrophil recruitment to lymph nodes limits local humoral response to *Staphylococcus aureus*. *PLoS Pathog.* **11**, e1004827 (2015).
9. T. Chtanova *et al.*, Dynamics of neutrophil migration in lymph nodes during infection. *Immunity* **29**, 487–496 (2008).
10. K. Brulois *et al.*, A molecular map of murine lymph node blood vascular endothelium at single cell resolution. *Nat. Commun.* **11**, 3798 (2020).
11. H. R. Hampton, J. Bailey, M. Tomura, R. Brink, T. Chtanova, Microbe-dependent lymphatic migration of neutrophils modulates lymphocyte proliferation in lymph nodes. *Nat. Commun.* **6**, 7139 (2015).
12. D. A. Rigby, D. J. Ferguson, L. A. Johnson, D. G. Jackson, Neutrophils rapidly transit inflamed lymphatic vessel endothelium via integrin-dependent proteolysis and lipoxin-induced junctional retraction. *J. Leukoc. Biol.* **98**, 897–912 (2015).
13. C. V. Gorlino *et al.*, Neutrophils exhibit differential requirements for homing molecules in their lymphatic and blood trafficking into draining lymph nodes. *J. Immunol.* **193**, 1966–1974 (2014).
14. L. S. C. Lok *et al.*, Phenotypically distinct neutrophils patrol uninfected human and mouse lymph nodes. *Proc. Natl. Acad. Sci. U.S.A.* **116**, 19083–19089 (2019).
15. A. B. Raff, D. Kroshinsky, Cellulitis: A review. *JAMA* **316**, 325–337 (2016).
16. G. J. Moran *et al.*; EMERGEncy ID Net Study Group, Methicillin-resistant *S. aureus* infections among patients in the emergency department. *N. Engl. J. Med.* **355**, 666–674 (2006).
17. T. R. Mempel, S. E. Henrickson, U. H. Von Andrian, T-cell priming by dendritic cells in lymph nodes occurs in three distinct phases. *Nature* **427**, 154–159 (2004).
18. S. Liao, P. Y. von der Weid, Inflammation-induced lymphangiogenesis and lymphatic dysfunction. *Angiogenesis* **17**, 325–334 (2014).
19. M. Jafarnejad, M. C. Woodruff, D. C. Zawieja, M. C. Carroll, J. E. Moore Jr., Modeling lymph flow and fluid exchange with blood vessels in lymph nodes. *Lymphat. Res. Biol.* **13**, 234–247 (2015).
20. K. Asano *et al.*, CD169-positive macrophages dominate antitumor immunity by crosspresenting dead cell-associated antigens. *Immunity* **34**, 85–95 (2011).
21. L. Martinez-Pomares, S. Gordon, CD169^{+} macrophages at the crossroads of antigen presentation. *Trends Immunol.* **33**, 66–70 (2012).
22. B. Ravishankar *et al.*, Marginal zone CD169+ macrophages coordinate apoptotic cell-driven cellular recruitment and tolerance. *Proc. Natl. Acad. Sci. U.S.A.* **111**, 4215–4220 (2014).
23. F. Pucci *et al.*, SCS macrophages suppress melanoma by restricting tumor-derived vesicle{\textendash}B cell interactions. *Science* **352**, 242–246 (2016).
24. M. Iannacone *et al.*, Subcapsular sinus macrophages prevent CNS invasion on peripheral infection with a neurotropic virus. *Nature* **465**, 1079–1083 (2010).
25. D. A. P. Louie, S. Liao, Lymph node subcapsular sinus macrophages as the frontline of lymphatic immune defense. *Front. Immunol.* **10**, 347 (2019).
26. M. Y. Gerner, K. A. Casey, W. Kastenmuller, R. N. Germain, Dendritic cell and antigen dispersal landscapes regulate T cell immunity. *J. Exp. Med.* **214**, 3105–3122 (2017).
27. J. E. Gretz, C. C. Norbury, A. O. Anderson, A. E. Proudfoot, S. Shaw, Lymph-borne chemokines and other low molecular weight molecules reach high endothelial venules via specialized conduits while a functional barrier limits access to the lymphocyte microenvironments in lymph node cortex. *J. Exp. Med.* **192**, 1425–1440 (2000).
28. J. E. Chang, S. J. Turley, Stromal infrastructure of the lymph node and coordination of immunity. *Trends Immunol.* **36**, 30–39 (2015).
29. R. Roozendaal *et al.*, Conduits mediate transport of low-molecular-weight antigen to lymph node follicles. *Immunity* **30**, 264–276 (2009).
30. M. Sixt *et al.*, The conduit system transports soluble antigens from the afferent lymph to resident dendritic cells in the T cell area of the lymph node. *Immunity* **22**, 19–29 (2005).
31. V. Ki, C. Rotstein, Bacterial skin and soft tissue infections in adults: A review of their epidemiology, pathogenesis, diagnosis, treatment and site of care. *Can. J. Infect. Dis. Med. Microbiol.* **19**, 173–184 (2008).
32. B. Silverberg, A structured approach to skin and soft tissue infections (SSTIs) in an Ambulatory Setting. *Clin. Pract.* **11**, 65–74 (2021).
33. A. H. Huang *et al.*, Real-world comorbidities of atopic dermatitis in the pediatric ambulatory population in the United States. *J. Am. Acad. Dermatol.* **85**, 893–900 (2021).
34. G. A. Noskin *et al.*, National trends in *Staphylococcus aureus* infection rates: Impact on economic burden and mortality over a 6-year period (1998-2003). *Clin. Infect. Dis.* **45**, 1132–1140 (2007).
35. T. Yamamoto *et al.*, Recurrent prosthetic valve endocarditis caused by Staphylococcus aureus colonizing skin lesions in severe atopic dermatitis. *Intern. Med.* **46**, 571–573 (2007).
36. P. H. Hoeger, R. Ganschow, G. Finger, Staphylococcal septicemia in children with atopic dermatitis. *Pediatr. Dermatol.* **17**, 111–114 (2000).
37. J. Choi *et al.*, Translational relevance of mouse models of atopic dermatitis. *J. Clin. Med.* **10**, 613 (2021).
38. M. Q. Man *et al.*, Characterization of a hapten-induced, murine model with multiple features of atopic dermatitis: Structural, immunologic, and biochemical changes following single versus multiple oxazolone challenges. *J. Invest. Dermatol.* **128**, 79–86 (2008).
39. S. E. Acton *et al.*, Dendritic cells control fibroblastic reticular network tension and lymph node expansion. *Nature* **514**, 498–502 (2014).
40. V. G. Martinez *et al.*, Fibroblastic reticular cells control conduit matrix deposition during lymph node expansion. *Cell Rep.* **29**, 2810–2822.e5 (2019).
41. S. Liao, N. H. Ruddle, Synchrony of high endothelial venules and lymphatic vessels revealed by immunization. *J. Immunol.* **177**, 3369–3379 (2006).
42. S. Liao *et al.*, Impaired lymphatic contraction associated with immunosuppression. *Proc. Natl. Acad. Sci. U.S.A.* **108**, 18784–18789 (2011).
43. Y. Lin *et al.*, Perinodal adipose tissue participates in immune protection through a lymphatic vessel-independent route. *J. Immunol.* **201**, 296–305 (2018).
44. R. E. Mebius, P. R. Streeter, J. Brevé, A. M. Duijvestijn, G. Kraal, The influence of afferent lymphatic vessel interruption on vascular addressin expression. *J. Cell Biol.* **115**, 85–95 (1991).
45. R. E. Mebius, J. Brevé, A. M. Duijvestijn, G. Kraal, The function of high endothelial venules in mouse lymph nodes stimulated by oxazolone. *Immunology* **71**, 423–427 (1990).
46. R. E. Mebius *et al.*, Expression of GlyCAM-1, an endothelial ligand for L-selectin, is affected by afferent lymphatic flow. *J. Immunol.* **151**, 6769–6776 (1993).
47. D. Aebischer, A. H. Willrodt, C. Halin, Oxazolone-induced contact hypersensitivity reduces lymphatic drainage but enhances the induction of adaptive immunity. *PLoS One* **9**, e99297 (2014).
48. U. H. von Andrian, C. M'Rini, In situ analysis of lymphocyte migration to lymph nodes. *Cell Adhes. Commun.* **6**, 85–96 (1998).
49. A. O. Anderson, N. D. Anderson, Studies on the structure and permeability of the microvasculature in normal rat lymph nodes. *Am. J. Pathol.* **80**, 387–418 (1975).
50. D. L. Drayton, S. Liao, R. H. Mounzer, N. H. Ruddle, Lymphoid organ development: From ontogeny to neogenesis. *Nat. Immunol.* **7**, 344–353 (2006).
51. B. G. Surewaard *et al.*, Identification and treatment of the *Staphylococcus aureus* reservoir in vivo. *J. Exp. Med.* **213**, 1141–1151 (2016).
52. G. J. Randolph, V. Angeli, M. A. Swartz, Dendritic-cell trafficking to lymph nodes through lymphatic vessels. *Nat. Rev. Immunol.* **5**, 617–628 (2005).
53. A. J. Radtke *et al.*, Lymph-node resident CD8α+ dendritic cells capture antigens from migratory malaria sporozoites and induce CD8+ T cell responses. *PLoS Pathog.* **11**, e1004637 (2015).
54. A. A. Tomei, S. Siegert, M. R. Britschgi, S. A. Luther, M. A. Swartz, Fluid flow regulates stromal cell organization and CCL21 expression in a tissue-engineered lymph node microenvironment. *J. Immunol.* **183**, 4273–4283 (2009).
55. J. E. Chang, M. B. Buechler, E. Gressier, S. J. Turley, M. C. Carroll, Mechanosensing by Peyer's patch stroma regulates lymphocyte migration and mucosal antibody responses. *Nat. Immunol.* **20**, 1506–1516 (2019).
56. D. Hoke *et al.*, Selective modulation of the expression of L-selectin ligands by an immune response. *Curr. Biol.* **5**, 670–678 (1995).
57. V. V. Swarte *et al.*, Regulation of fucosyltransferase-VII expression in peripheral lymph node high endothelial venules. *Eur. J. Immunol.* **28**, 3040–3047 (1998).
58. K. Veerman, C. Tardiveau, F. Martins, J. Coudert, J. P. Girard, Single-cell analysis reveals heterogeneity of high endothelial venules and different regulation of genes controlling lymphocyte entry to lymph nodes. *Cell Rep.* **26**, 3116–3131.e5 (2019).